Supplementary Information for

Hepatic gap junctions amplify alcohol liver injury by propagating cGAS-mediated IRF3 activation

Jay Luther, Sanjoy Khan, Manish K. Gala, Dmitry Kedrin, Gautham Sridharan, Russell P. Goodman, John J. Garber, Ricard Masia, Erik Diagacom, Daniel Adams, Kevin R. King, Samuel Piaker, Hans-Christian Reinecker, Martin L. Yarmush, Josepmaria Argemi, Ramon Bataller, Jules L. Dienstag, Raymond T. Chung, Suraj J. Patel

Suraj J. Patel
Email: sjpatel32@mgh.harvard.edu

This PDF file includes:

Supplementary text
Figures S1 to S10
SI References

www.pnas.org/cgi/doi/10.1073/pnas.1911870117

Supplementary Information Text

METHODS:

Biochemical analysis of liver injury

Immediately following euthanasia, systemic blood was collected from the inferior vena cava of the mice. Serum was obtained by centrifugation of whole blood at 10,000 rpm for 10 minutes. To determine the extent of hepatocyte injury, quantification of alanine aminotransferase (ALT) and aspartate aminotransferase (AST) was performed from serum using the Infinity™ ALT and AST Liquid Stable Reagant (Thermo Scientific, Middletown, Virginia).

Histological analysis of hepatic steatosis and inflammation

The intact liver was excised immediately after mouse sacrifice, fixed in formalin for 24 hours, and then embedded in paraffin. Histological analysis was performed on liver sections stained with hematoxylin and eosin (H&E). Examination was performed in a blinded fashion by one hepatopathologist (RM) and one hepatologist (JL). A modified version of the Brunt classification was used to objectively assess hepatic injury, given the lack of hepatocyte ballooning observed in mice. Specifically, histological specimens were scored at 20X for steatosis (<25%:1 point, 25-50%: 2 points, 50-75%: 3 points, and >75%: 4 points) and inflammation (1 foci of inflammation: 1 point, 2 or greater foci of inflammation: 2 points). The steatosis and inflammation score were added together to give a total histological score (1).

Serum ethanol measurement

Serum was collected from the inferior vena cava, and ethanol levels were measured using the Ethanol Assay Kit (Abcam, Cambridge, MA).

Quantitative real-time polymerase chain reaction

Mouse liver tissues were mechanically homogenized using the PowerGen 125 Homogenizer (Fisher Scientific, USA). Total RNA was extracted using the RNeasy Mini Kit® (Qiagen, Valencia, California). Total RNA (500 nanograms) was converted into cDNA using the RT^2 First Strand Kit (SA Biosciences, Valencia, California). Quantitative RT-PCR was performed using the RT^2 Master Mix Kit (SA Biosciences, Valencia, California, USA) and the iQ™5 system (Bio-Rad, Hercules, California). Quantitative RT-PCR was performed for mRNA expression using primers designed by SA Biosciences (Qiagen, Valencia, California). Expression of a house keeping gene (*GAPDH, β-actin, 16S rRNA)* was used to standardize the samples, and the results are expressed as a ratio relative to control.

Cytosolic mitochondrial DNA quantification

Hepatocytes were isolated from liver tissue as previously described (2). Following hepatocyte isolation, fractionation of the nuclear, mitochondrial, and cytosolic fractions was performed using a cell fractionation kit (Abcam, Cambridge, MA, USA). DNA was then isolated from the pure cytosolic fraction supernatant using QIAQuick Nucleotide Removal Columns (Qiagen, Germany). Quantification of mitochondrial DNA was performed using quantitative PCR of Dloop 1, 2, and 3. Levels of mtDNA from whole-cell extracts served as normalization controls for the mtDNA values obtained from the cytosolic fractions (3,4).

Hepatocyte co-culture experimentation

Donor H35 hepatocytes were transfected with 2'3'-cGAMP (Invivogen). Two hours after stimulation, donor cells were trypsinized, washed three times in PBS, and counted. 2'3'-cGAMP-stimulated donor cells were then transplanted onto a sub-confluent layer of recipient IRF3-GFP reporters, maintaining a 1:10 ratio between donor and recipient cells. After 18 h of coculture, recipient reporter cells were analyzed by fluorescent microscopy and FACS for IRF3 activity.

Hepatic triglyceride measurements

To determine the abundance of lipid droplets in liver specimens, we stained frozen hepatic tissue with Oil Red O, as previously described (5). Furthermore, to determine the concentration of hepatic triglycerides, we used a colorimetric triglyceride quantification kit (Abcam, Cambridge, MA).

Microarray Analysis

Isolated liver mRNA was used for hepatic mRNA microarray analysis on the Affymetrix GeneChip Mouse Gene ST 2.0 platform (Affymetrix Inc., Santa Clara, CA). Analysis was performed as previously described (6).

Metabolomics Analysis

Liver tissue extraction for metabolite analysis was performed as previously described (7). Briefly, 15 mg of liver tissue was collected and flash frozen in liquid nitrogen. The tissue was then smashed with a pestle upon the addition of methanol. A series of methanol extractions, centrifugations, and supernatant collection steps ensued, and the final extract was lyophilized to a pellet, which was sent to a metabolomics core for metabolomics analysis. The analysis entailed multiple reaction monitoring (MRM) using an AB Sciex 5500 QTRAP liquid-chromatography tandem mass spectrometer

(LC/MS-MS) instrument, where 258 unique metabolites from 289 Q1/Q3 precursor/product ion transitions were quantified by chromatographic peak area and provided to us as raw data. The data were then further processed for statistical analysis. Each MRM peak area for a metabolite was normalized to the sum of all the MRM peak areas for a particular sample to account for differences in initial tissue mass and extraction efficiency.

For principal component analysis (PCA), the data matrix was created by first removing all metabolites from the normalized data, for which at least one entry was assigned 'N/A', meaning that there was no quantifiable peak for that MRM transition in that sample extract. Next, each entry in the matrix was replaced by a z-score to represent the relative value of the entry compared to the distribution of normalized peak areas across the 16 samples. This was done to prevent certain metabolites with higher nominal values from dominating in contribution to the principal components.

Immunoblotting

Mouse liver tissues were lysed in RIPA lysis buffer (Santa Cruz Biotechnology Inc.; catalog sc-24948) containing protease inhibitor cocktail. Lysates were clarified by centrifuging at 12,000 rpm for 10 min at 4°C, and protein concentration was determined by Bradford assay. The boiled samples were separated on Bis-Tris protein gels and transferred to nitrocellulose membranes (Life Technologies, Thermo Fisher Scientific). After blocking with 5% nonfat milk or BSA in Tris-Buffered Saline with 0.1% Tween-20 for 1 hour, the membranes were probed with the corresponding antibodies overnight. Bound antibodies were visualized by ECL (EMD Millipore or Pierce, Thermo Fisher Scientific) using HRP-conjugated secondary antibodies. Anti-cGAS (#31659), anti-IRF3 (#4302), anti-pIRF3 (#29047) and anti-TBK1 (#3504) antibodies were purchased from Cell Signaling Technology. Anti-GAPDH (SAB1405848) was purchased from Sigma-

Aldrich. Anti-mouse and anti-rabbit HRP-conjugated secondary antibodies were purchased from GE Healthcare Life Science.

In vivo transfection experiments

WT mice were injected via the tail vein with an adenoviral construct containing GDPD3 and GFP, or a GFP alone control to induce GDPD3 over-expression (SignaGen Laboratories, Rockland, MD). These mice were then exposed to a modified version of the chronic and binge ethanol model, in which mice were injected on day 9 with either a recombinant adenoviral vectors expressing GDPD3-GFP (GDPD3) or GFP alone (GFP). Mice were then gavaged with 5 grams of ethanol per kilogram of body weight on day 12 and sacrificed 9 hours later.

2-Aminoethoxydiphenyl Borate (2APB) treatment in vivo

2APB (Sigma Aldrich) was made fresh for each experiment in DMSO (200 mg/ml) as a vehicle. 2APB was dosed at 20 mg/kg prior to the oral gavage in the acute-on-chronic ethanol binge experiments. In the survival experiment, 2-APB was dosed at the same concentration but at a frequency of every 24 hours. All vehicle control mice received the same volume of DMSO (0.1 mL/kg) used to dissolve 2APB.

Primary human hepatocytes

Primary human hepatocytes (PHH) were obtained from the NIH-sponsored Liver Cell Tissue Distribution System at the University of Pittsburgh (courtesy of Shadi Salloum of Dr. Raymond Chung's laboratory). The hepatocytes were obtained from a 66-year-old woman who underwent a wedge liver resection as part of her treatment for metastatic colorectal cancer to the liver. The patient did also receive chemotherapy. PHHs were cultured overnight in DMEM media on a collagen-coated plate. The following

day, the media was replaced with an ethanol-supplemented media to a concentration of 500mM. After 24 hours, the PHHs were collected, mRNA was isolated, and qPCR was performed.

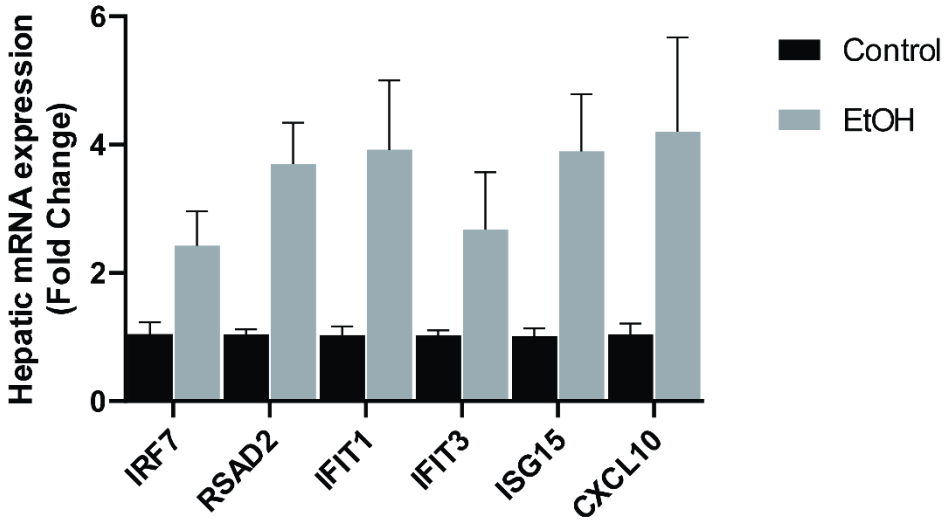

Supp. Fig. 1. *In vitro* alcohol exposure induces the cGAS-IRF3 pathway in primary human hepatocytes.

Primary human hepatocytes (PHHs) were obtained from the NIH-sponsored Liver Cell Tissue Distribution System at the University of Pittsburgh. PHHs were isolated from normal hepatic tissue included from a wedge resection from a patient with metastatic colorectal cancer to the liver. Upon receipt, PHHs were cultured in control media or media containing 500mM ethanol for 24 hours, after which time cells were harvested and mRNA expression was quantified using RT-PCR. * $P < 0.05$; ** $P < 0.01$; *** $P < 0.001$.

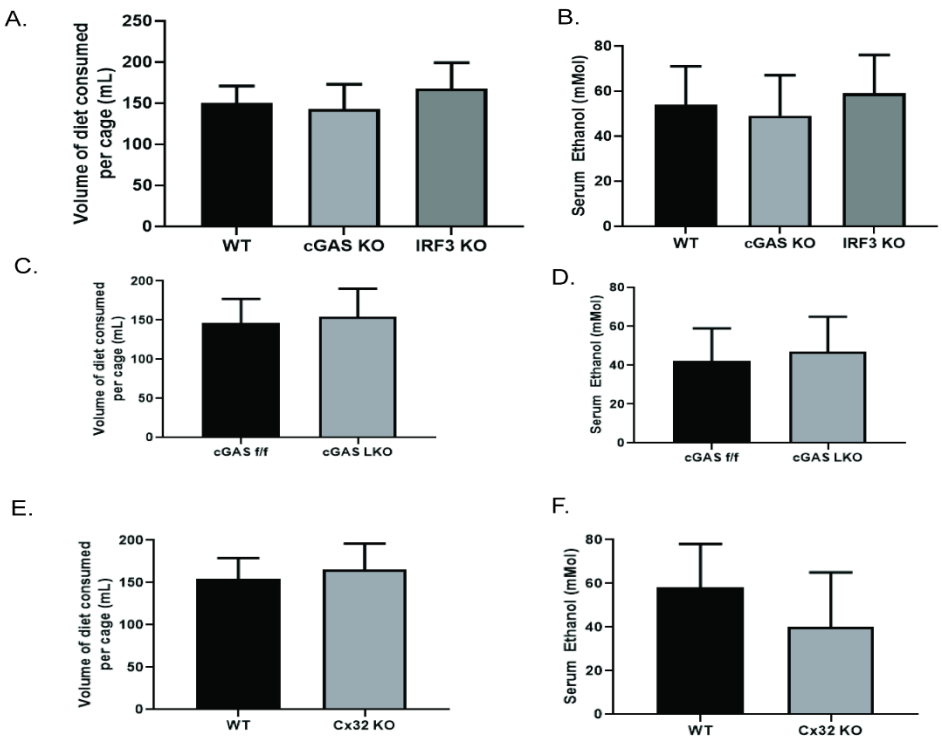

Supp. Fig. 2. Alcohol consumption and serum levels during the NIAAA chronic and binge model

Wild-type (WT), cGAS-deficient mice (cGAS KO), IRF3-deficienct mice (IRF3 KO), hepatocyte-specific cGAS-deficient mice (cGAS LKO), floxed cGAS mice (cGAS f/f), and connexin 32-deficient (Cx32 KO) mice were exposed to 10 days of 5% ethanol followed by a single binge of ethanol. (A, C, E) The total volume of ethanol-containing diet consumed during the 10 days excluding the binge. (B, D, F) The serum ethanol levels found in mice at the time of sacrifice.

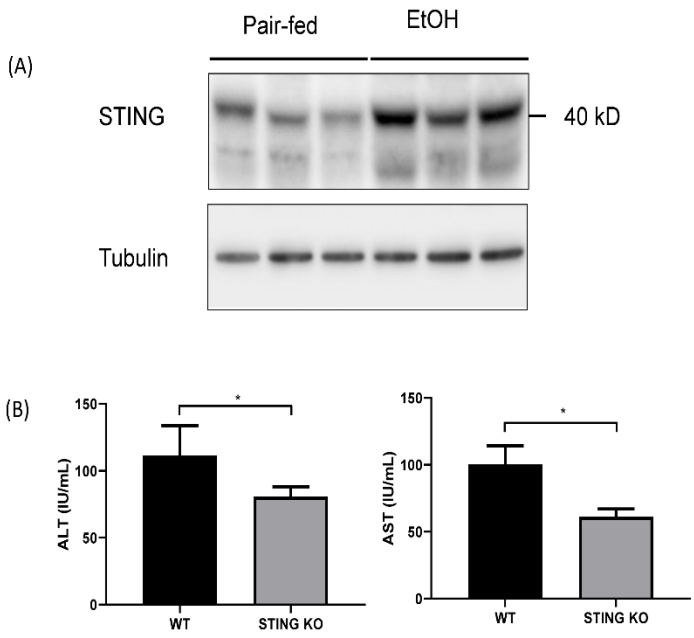

Supp. Fig. 3. STING deficiency protects against alcohol-induced liver injury in mice.

Wild-type (WT) mice were exposed to one binge of ethanol, 4 hours after which liver tissue and serum were collected. (A) Immunoblot for STING from hepatic tissue of WT mice fed a control or ethanol binge. (B) WT and STING-deficient mice (STING KO) mice we exposed to one binge of ethanol. 4 hours after the binge, mice were sacrificed and serum measurements of ALT and AST were performed. N = 6 mice per group. * $P < 0.05$; ** $P < 0.01$; *** $P < 0.001$.

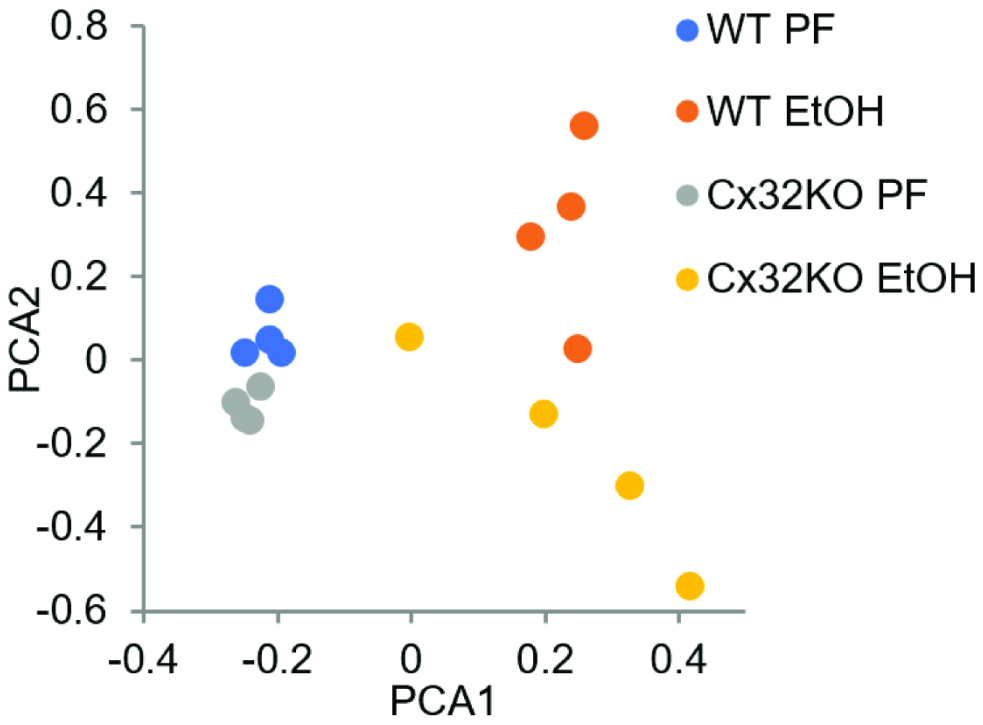

Supp. Fig. 4. Differential metabolomic profiling from WT and Cx32KO mice. Principle component analyses (PCA) of hepatic metabolites from WT and connexin 32-deficient (Cx32 KO) mice exposed to ethanol suggest that there were distinct responses to ethanol dependent on the presence or absence of Cx32.

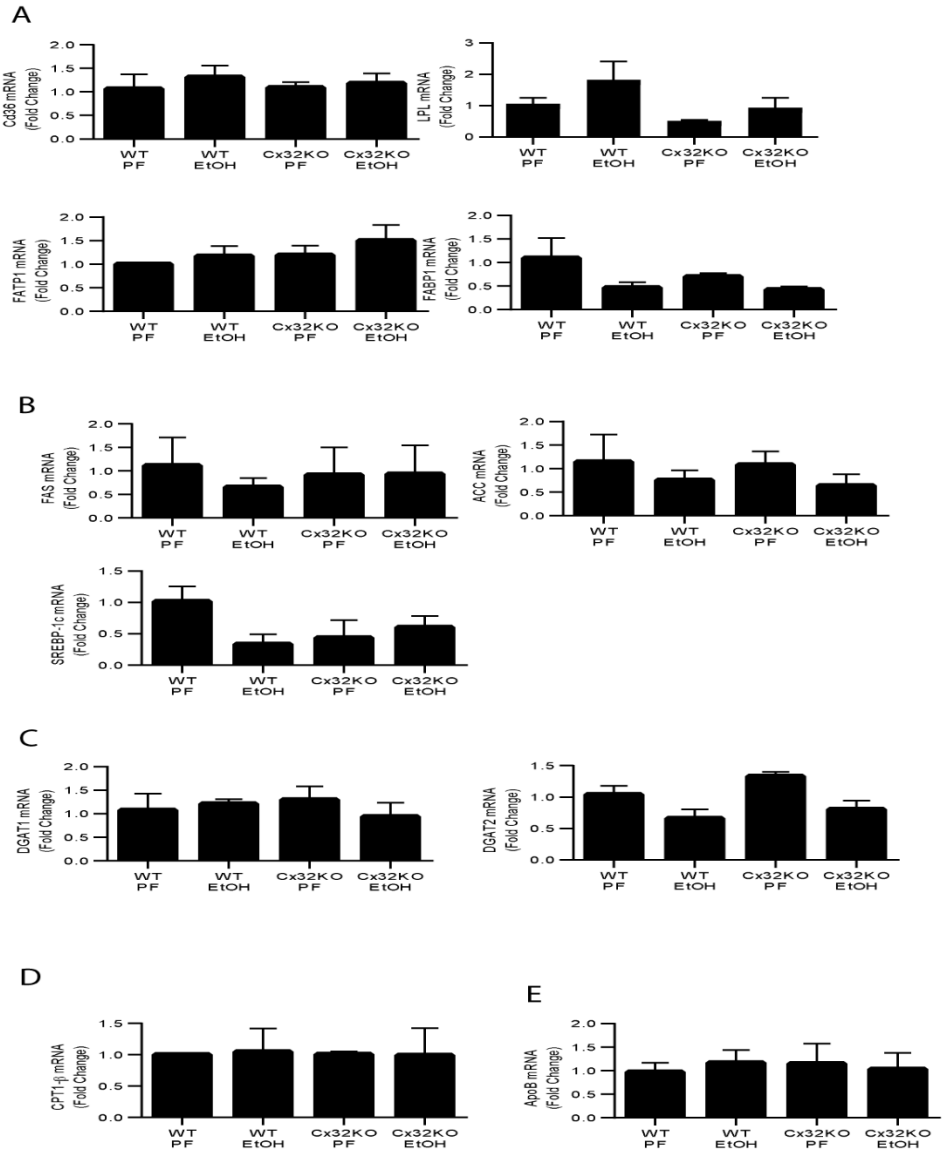

Supp. Fig. 5. Connexin 32 deficiency does not induce transcriptional changes in classic lipid metabolism genes

Wild-type (WT) and connexin 32-deficient (Cx32 KO) mice were exposed to 10 days of 5% ethanol followed by a single binge of ethanol. RT-PCR was performed to measure hepatic gene expression of genes involved in (A) fatty acid uptake, (B) de novo lipogenesis, (C) triglyceride synthesis, (D) fatty acid oxidation, and (E) lipid transport. Data are normalized to the expression of each gene seen in the WT PF group. PF = pairfed; EtOH = alcohol.

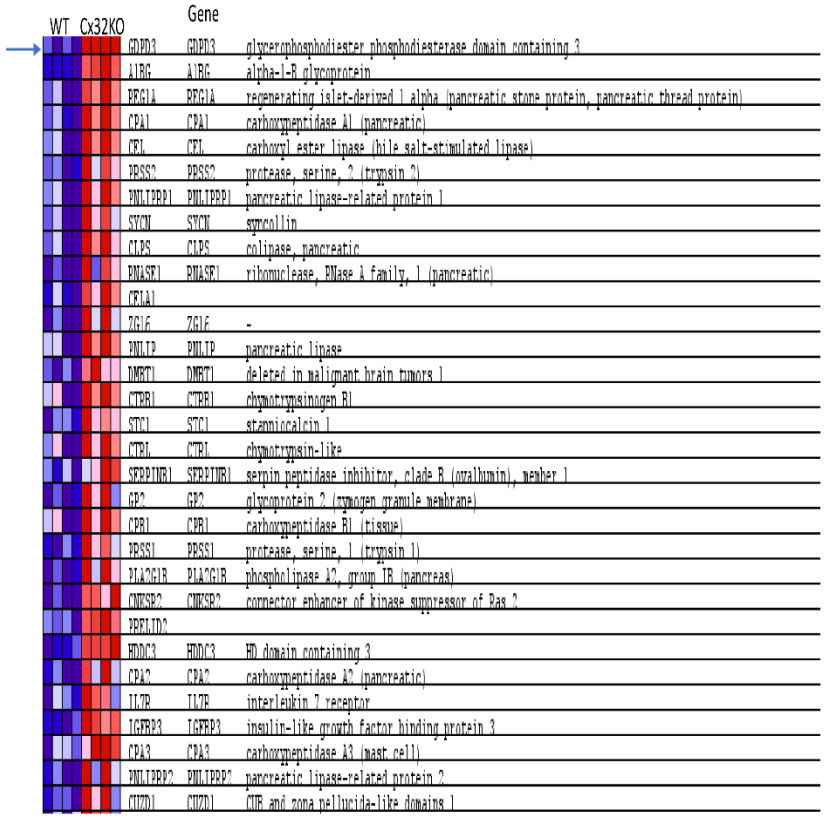

Supp. Fig. 6. GDPD3 is the most upregulated hepatic gene in Cx32 KO mice

Heatmap representation of genes differentially expressed in the liver based on Cx32 genotype. Red indicates relative increased expression and blue indicates relative decreased expression. The arrow highlights Glycerophosphodiester phosphodiesterase domain containing 3 (GDPD3), the most significantly upregulated gene in the Cx32 KO mice based on P-value (3.2 x 10-8).

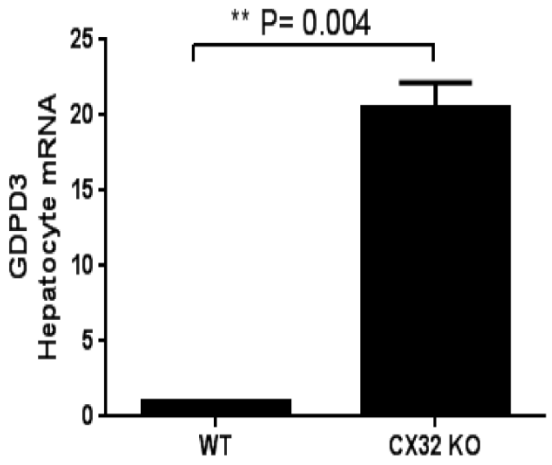

Supp. Fig. 7. GDPD3 expression localizes to hepatocytes in Cx32 KO mice.

Hepatocytes were isolated from Cx32 KO mice exposed to alcohol. mRNA was isolated and the expression of GDPD3 was quantified using RT-PCR.

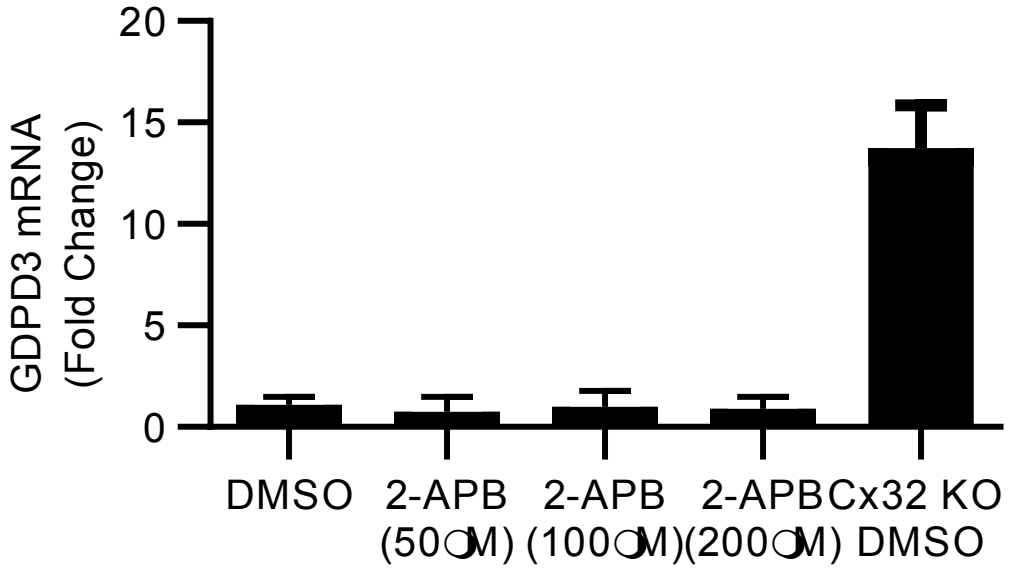

Supp. Fig. 8. Treatment with 2-APB does not affect GDPD3 expression.

Primary murine hepatocytes treated with supraphysiological doses of 2-APB or control for 24 hours, after which mRNA was isolated and assessed for GDPD3 expression. Primary murine hepatocytes isolated from Connexin 32-deficient mice (Cx32 KO) were also treated with DMSO, after which GDPD3 expression was assessed.

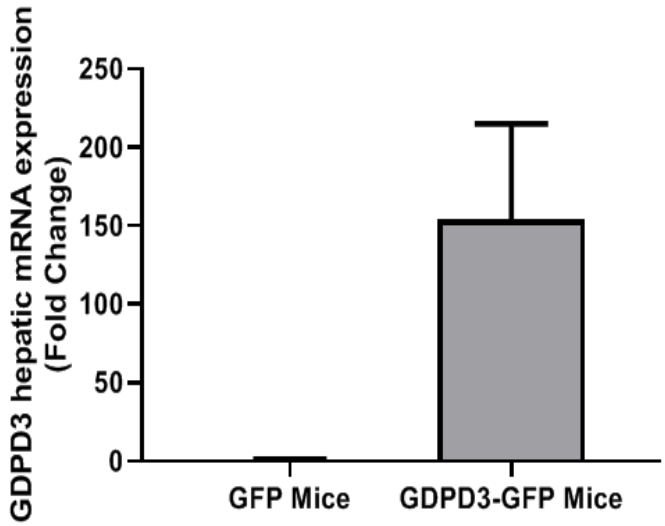

Supp. Fig. 9. Upregulation of hepatic GDPD3 in GDPD3-GFP-treated mice.

Measurement of hepatic mRNA expression of GDPD3 in GDPD3-GFP and GFP mice. The difference is statistical significant ($P < 0.05$).

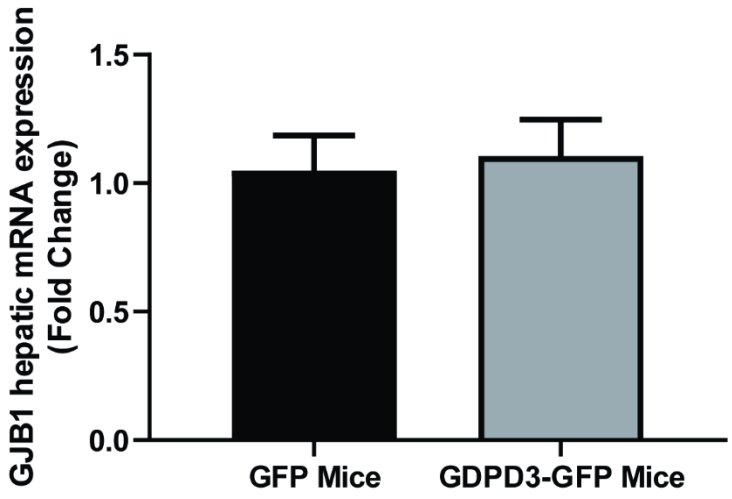

Supp. Fig. 10. GJB1 expression was not altered in GDPD3-overexpressing mice.

mRNA expression of GJB1, the gene that encodes connexin 32, from hepatic tissue of GDPD3 and control mice.

References

1. Uesugi T, et al, Role of lipopolysaccharide-binding protein in early alcohol-induced liver injury in mice. J Immunol 168(6), 2963-9 (2002).

2. Houseman L, et al, Isolation and culture of mouse hepatocytes: gender-specific gene expression responses to chemical treatments. Methods Mol Biol 1250, 3-12 (2015).

3. West AP, et al, Mitochondrial DNA stress primes the antiviral innate immune response. Nature 520(7548), 533-7 (2015).

4. Bai J, et al, DsbA-L prevents obesity-induced inflammation and insulin resistance by suppressing the mtDNA release-activated cGAS-cGAMP-STING pathway. Proc Natl Acad Sci USA 114(46), 12196-12201 (2017).

5. Mehlem A, et al, Imaging of neutral lipids by oil red O for analyzing the metabolic status in health and disease. Nat Protoc 8(6), 1149-54 (2013).

6. Luther J, et al, Hepatic connexin 32 associates with nonalcoholic fatty liver disease severity. Hepatol Commun 2(7), 786-797 (2018).

7. Yuan M, et al, A positive/negative ion-switching, targeted mass spectrometry-based metabolomics platform for bodily fluids, cells, and fresh and fixed tissue. Nat Protoc 7(5), 872-81 (2012)